

Structure Determination of LISICON Solid Solutions by Powder Neutron Diffraction

I. ABRAHAMS AND P. G. BRUCE*

Department of Chemistry, Heriot-Watt University, Riccarton, Edinburgh EH14 4AS, Scotland, United Kingdom

A. R. WEST

Department of Chemistry, University of Aberdeen, Meston Walk, Old Aberdeen AB9 2UE, Scotland, United Kingdom

AND W. I. F. DAVID

Rutherford-Appleton Laboratory, SERC, Chilton, Didcot, Oxon OX11 0QX, United Kingdom

Received October 23, 1987

The structures of $\text{Li}_3\text{Zn}_{0.5}\text{GeO}_4$ and $\text{Li}_{3.5}\text{Zn}_{0.25}\text{GeO}_4$ have been determined by powder neutron diffraction studies at room temperature. Both compounds are members ($x = 0.5$, $x = 0.75$) of the LISICON solid solution series $\text{Li}_{(2+2x)}\text{Zn}_{(1-x)}\text{GeO}_4$ where $-0.36 \leq x \leq 0.87$. The structures, which are essentially similar, have been solved in the orthorhombic space group *Pnma* (No. 62) with cell dimensions $a = 10.8720(5)$, $b = 6.2882(3)$, and $c = 5.1696(2)$ Å for $\text{Li}_3\text{Zn}_{0.5}\text{GeO}_4$ and $a = 10.8845(7)$, $b = 6.2683(4)$, and $c = 5.1551(2)$ Å for $\text{Li}_{3.5}\text{Zn}_{0.25}\text{GeO}_4$; $Z = 4$. The basic structure of both compounds consists of an oxide ion array that is intermediate between hexagonal close packing and tetragonal packing, with Ge, Zn, and Li located in tetrahedral sites between the oxide ions. Additional Li is located in octahedral interstices which share faces with adjacent tetrahedral sites: Li ions in these tetrahedral sites are repelled through their faces to more distant tetrahedral sites. © 1988 Academic Press, Inc.

Introduction

In the search for fast lithium ion conducting solid electrolytes, the solid solution system $\text{Li}_{(2+2x)}\text{Zn}_{(1-x)}\text{GeO}_4$ where $-0.36 \leq x \leq 0.87$ has received considerable attention. Only the lithium-rich solid solutions ($x > 0$)

exhibit high ionic conductivity. One member of this series, $\text{Li}_{14}\text{Zn}(\text{GeO}_4)_4$ ($x = 0.75$), was first investigated by Hong (1) who reported that it possessed a conductivity of $0.13 \text{ ohm}^{-1} \text{ cm}^{-1}$ at 300°C ; this is among the best lithium ion conductivity at this temperature yet discovered. Hong named this compound LISICON from which the entire solid solution series has derived its name.

* To whom correspondence should be addressed.

Subsequently, Bruce and West carried out a detailed investigation of the binary phase diagram $\text{Li}_4\text{GeO}_4\text{-Zn}_2\text{GeO}_4$ encompassing the LISICON solid solution (2) and the variation of conductivity with composition (3, 4). Two single-crystal X-ray structure determinations have been carried out on these solids, one on the $x = 0.75$ composition, by Hong (1), and the other on the composition $x = 0.5$, by Plattner and Völlenknecht (5). Both structure determinations agree on the zinc germanate framework, but are in disagreement concerning the lithium ion distribution; this may reflect a genuine structural difference, or, alternatively, may signal that X-ray techniques are inadequate for the determination of the lithium arrangement in these compounds. Compared with Zn, Ge, and O, Li is a weak scatterer of X-rays; however, ^7Li scatters neutrons strongly. For this reason we chose to determine the structure of two LISICON solid solutions, $x = 0.5$ and $x = 0.75$, by powder neutron diffraction with the particular goal of determining the lithium ion distribution. This information is vital to an understanding of the mechanism of lithium ion transport in these systems.

Experimental

Preparation

$\text{Li}_3\text{Zn}_{0.5}\text{GeO}_4$ and $\text{Li}_{3.5}\text{Zn}_{0.25}\text{GeO}_4$ were prepared by solid-state reaction from $^7\text{Li}_2\text{CO}_3$, GeO_2 , and ZnO , as described previously (2).

Data Collection

Powder neutron diffraction profiles were obtained at a constant wavelength of 1.909 Å on the DIA diffractometer at the ILL (Grenoble). Data were collected from 6 to 160° in 2θ and in steps of 0.05°. Structure analysis was performed by profile refinement using the Rietveld method (6). The scattering lengths used were: $^7\text{Li} = -0.220$,

$\text{Ge} = 0.819$, $\text{Zn} = 0.569$, $\text{O} = 0.580$, $\text{C} = 0.665 \times 10^{-12}$ cm (7, 8).

Structure Determination

A similar approach was adopted for the structure determinations of both the $x = 0.5$ and 0.75 compositions: below, we describe this approach for the $x = 0.5$ composition.

$\text{Li}_3\text{Zn}_{0.5}\text{GeO}_4$

The powder pattern for this compound (Fig. 1) could be indexed on the orthorhombic cell of space group $Pnma$ (No. 62 (9)), as determined by the single-crystal X-ray studies. However, a detailed examination of the neutron profile revealed several small peaks that could not be indexed on this orthorhombic cell. In general these peaks appeared only as shoulders on the LISICON peaks. The additional reflections could be indexed on the monoclinic unit cell of Li_2CO_3 (10). It is known that prolonged exposure to air can lead to slight decomposition of LISICON solid solutions with the formation of lithium carbonate. Although the peaks in the neutron profile arising from this compound constitute only a minor part of the profile, it is necessary to take account of these if a detailed structure refinement is to be obtained. We have therefore, refined the neutron profiles using a version of the multipattern Rietveld code (11, 12). Two hundred thirty six reflections from the primary phase and 14 reflections from the secondary phase were included in the refinement. Further secondary phase reflections were too low in intensity to significantly influence the profile. During refinement, only the scale factor and lattice parameters for $^7\text{Li}_2\text{CO}_3$ were refined simultaneously with the LISICON phase parameters, since the structure of lithium carbonate is not in doubt.

In the initial refinement only the heavy atoms (Ge, O, Zn) were included; their occupancies were fixed at the values given in

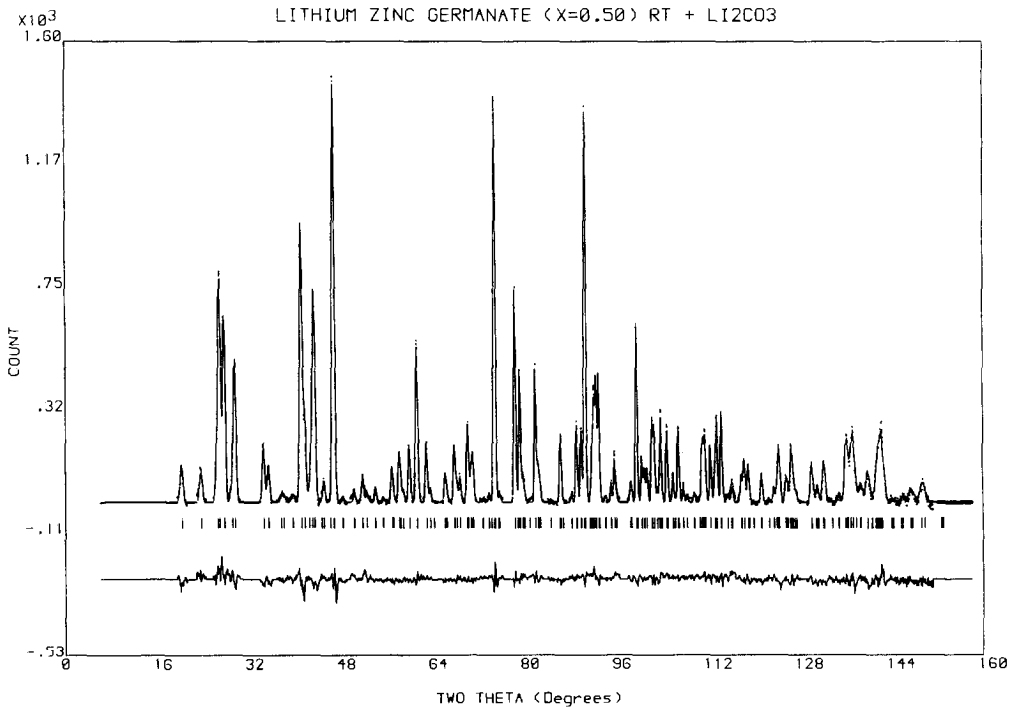


FIG. 1. Observed (points), calculated (solid line), and difference powder neutron profiles for $\text{Li}_3\text{Zn}_{0.5}\text{GeO}_4$. Bragg peaks are indicated by solid vertical lines.

Ref. (5), from which the initial positional parameters were also obtained. The scale factor, zero point correction, half-width parameters, and cell dimensions were refined first without varying the atomic parameters. The heavy atom positions were then allowed to refine and a difference Fourier map was generated; this allowed identification of the lithium positions within the unit cell. In this way three Li atoms were initially located in the following positions:

Site	x/a	y/b	z/c
Li(1)	4c	0.42	0.75 0.17
Li(2)	8d	0.17	0.00 0.30
Li(2a)	8d	0.20	0.00 0.12

Li(1) and Li(2) share their sites with Zn(1) and Zn(2), respectively. These positions were incorporated into the model and then refined along with their site occupancies. A second difference Fourier map was subse-

quently generated from this, which indicated the existence of a further lithium site:

Site	x/a	y/b	z/c
Li(3)	4c	0.22	0.25 0.00

B factors for Ge and O atoms refined satisfactorily; however, it proved impossible to refine individually the isotropic B factors on the Li/Zn(1), Li/Zn(2), Li(2a), and Li(3) sites. A single B factor was therefore assigned to all lithium and zinc ions; this was refined along with the lithium site occupancies. It is noteworthy that this refinement indicated a total occupancy of unity for lithium and zinc ions on site(1) and that the total number of lithium and zinc ions distributed over the (2) and (2a) sites was also unity. In the final refinement the Zn^{2+} occupancies were allowed to vary between sites (1) and (2) with the total Zn^{2+} content being

TABLE I

REFINED CELL AND ATOMIC PARAMETERS FOR
 $\text{Li}_3\text{Zn}_{0.5}\text{GeO}_4$ (WITH ESTIMATED STANDARD
 DEVIATIONS IN PARENTHESES)

$a = 10.8720(5) \text{ \AA}, b = 6.2882(3) \text{ \AA}, c = 5.1696(2) \text{ \AA}$						
Atom	Pos.	x/a	y/b	z/c	$B (\text{\AA}^2)$	occ
Ge	4c	0.4138(6)	0.25	0.3303(9)	0.97(9)	1
O(1)	8d	0.3363(6)	0.0227(7)	0.215(1)	1.3(1)	1
O(2)	4c	0.0876(8)	0.75	0.170(1)	1.0(1)	1
O(3)	4c	0.0646(7)	0.25	0.285(1)	1.0(1)	1
Li(1)	4c	0.429(4)	0.75	0.168(7)	2.1(8)	0.89(3)
Zn(1)	4c	0.429(4)	0.75	0.168(7)	2.1(8)	0.11(3)
Li(2)	8d	0.134(10)	-0.007(19)	0.325(29)	2.1(8)	0.63(1)
Zn(2)	8d	0.134(10)	-0.007(19)	0.325(29)	2.1(8)	0.20(1)
Li(2a)	8d	0.151(8)	0.006(13)	0.153(19)	2.1(8)	0.17(2)
Li(3)	4c	0.202(6)	0.25	0.037(14)	2.1(8)	0.27(5)

fixed at the value determined by the composition of the solid.

The final refinement terminated with $R_{\text{wp}} = 8.24\%$ and $R_e = 5.7\%$ (for definition of R factors see Ref. (6)). The final refined atomic parameters for $\text{Li}_3\text{Zn}_{0.5}\text{GeO}_4$ are given in Table I; the bond lengths derived from these are given in Table II. Examination of Table II reveals some abnormally short lithium-oxygen bond lengths, for example $\text{Li}(2a)\text{-O}(2) = 1.76(4) \text{ \AA}$ (typically, tetrahedral Li-O bonds range from 1.88–2.10 \AA). However, it is also evident that these bond lengths have particularly high e.s.d.s sufficiently so to reach more normal bond lengths within 2 e.s.d.s (1.92 \AA for $\text{Li}(2a)\text{-O}(2)$ within 2 e.s.d.s). The high e.s.d.s indicate considerable positional/thermal disorder in these sites.

$\text{Li}_{3.5}\text{Zn}_{0.25}\text{GeO}_4$

The powder neutron pattern of this more lithium-rich compound (Fig. 2) indicates higher levels of ${}^7\text{Li}_2\text{CO}_3$. Two hundred thirty three reflections of the primary phase and 44 of the secondary were included in the refinement. The structure is broadly similar to that of $\text{Li}_3\text{Zn}_{0.5}\text{GeO}_4$ with of course a lower zinc and higher lithium content. In this case refinement indicated that a small amount of additional lithium may be

TABLE II

BOND LENGTHS AND SIGNIFICANT CONTACT
 DISTANCES (\AA) FOR $\text{Li}_3\text{Zn}_{0.5}\text{GeO}_4$ (WITH ESTIMATED
 STANDARD DEVIATIONS IN PARENTHESES)

Ge-O(1)	1.763(6)	Li(1)/Zn(1)-O(1)	2.00(2)
Ge-O(1')	1.763(6)	Li(1)/Zn(1)-O(1')	2.00(2)
Ge-O(2)	1.757(8)	Li(1)/Zn(1)-O(2)	1.92(4)
Ge-O(3)	1.744(9)	Li(1)/Zn(1)-O(3)	1.98(4)
Mean	1.76	Mean	1.98
Li/Zn(2)-O(1)	2.05(15)	Li(2a)-O(1)	2.28(10)
Li/Zn(2)-O(1')	2.28(11)	Li(2a)-O(1')	2.04(9)
Li/Zn(2)-O(2)	1.80(13)	Li(2a)-O(2)	1.76(8)
Li/Zn(2)-O(3)	1.80(12)	Li(2a)-O(3)	1.92(9)
Mean	1.98	Mean	2.00
	Li(3)-O(1)	2.24(5)	
	Li(3)-O(1')	2.24(5)	
	Li(3)-O(3)	1.97(7)	
	Li(3)-O(1'')	2.43(5)	
	Li(3)-O(1''')	2.43(5)	
	Li(3)-O(2)	2.97(7)	

accommodated in the interstitial position Li(4):

Site	x/a	y/b	z/c
Li(4)	4b	0.00	0.50

The final refined parameters are given in Table III with the derived bond lengths given in Table IV. For this model the R factors were $R_{\text{wp}} = 11.35\%$ and $R_e = 5.2\%$. The larger weighted profile R factor for $x =$

TABLE III

REFINED CELL AND ATOMIC PARAMETERS FOR
 $\text{Li}_{3.5}\text{Zn}_{0.25}\text{GeO}_4$ (WITH ESTIMATED STANDARD
 DEVIATIONS IN PARENTHESES)

$a = 10.8845(7) \text{ \AA}, b = 6.2683(4) \text{ \AA}, c = 5.1551(2) \text{ \AA}$						
Atom	Pos.	x/a	y/b	z/c	$B (\text{\AA}^2)$	occ
Ge	4c	0.4127(6)	0.25	0.341(1)	1.0(1)	1
O(1)	8d	0.3364(6)	0.0206(8)	0.222(1)	1.7(1)	1
O(2)	4c	0.0883(9)	0.75	0.181(2)	1.6(2)	1
O(3)	4c	0.0632(7)	0.25	0.273(2)	1.1(2)	1
Li(1)	4c	0.430(4)	0.75	0.186(8)	2.7(6)	0.92(3)
Zn(1)	4c	0.430(4)	0.75	0.186(8)	2.7(6)	0.08(3)
Li(2)	8d	0.160(3)	-0.011(6)	0.358(9)	2.7(6)	0.68(1)
Zn(2)	8d	0.160(3)	-0.011(6)	0.358(9)	2.7(6)	0.08(2)
Li(2a)	8d	0.169(7)	0.043(11)	0.184(16)	2.7(6)	0.24(3)
Li(3)	4c	0.208(7)	0.25	-0.055(11)	2.7(6)	0.34(5)
Li(4)	4b	0.0	0.0	0.5	2.7(6)	0.06(4)

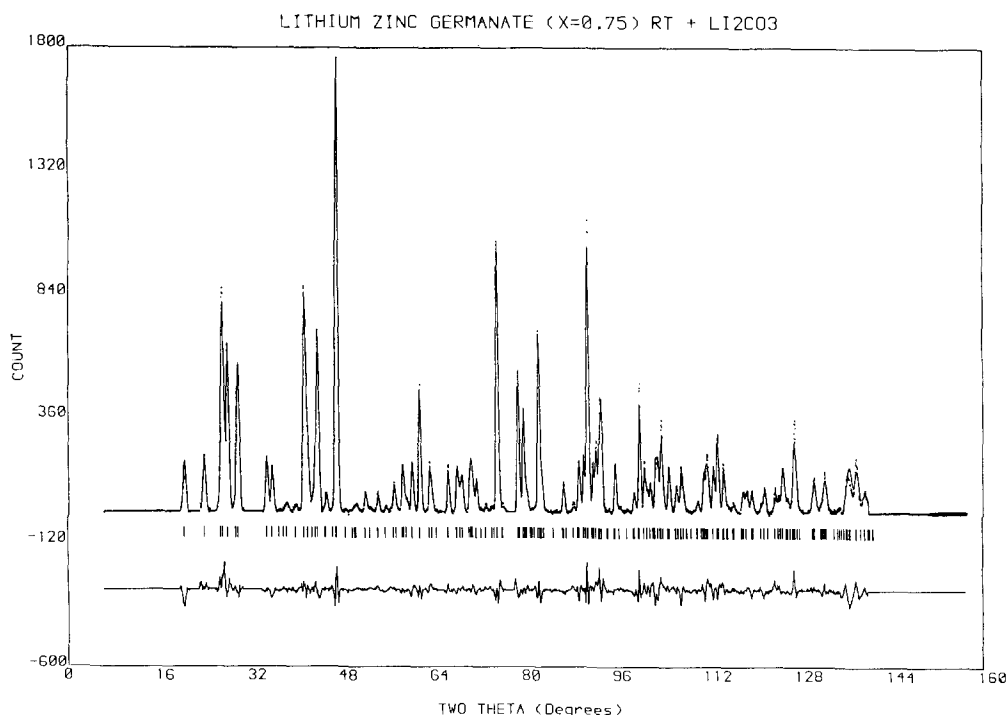


FIG. 2. Observed (points), calculated (solid line), and difference powder neutron profiles for $\text{Li}_{3.5}\text{Zn}_{0.25}\text{GeO}_4$. Bragg peaks are indicated by solid vertical lines.

TABLE IV
BOND LENGTHS AND SIGNIFICANT CONTACT
DISTANCES (Å) FOR $\text{Li}_{3.5}\text{Zn}_{0.25}\text{GeO}_4$ (WITH
ESTIMATED STANDARD DEVIATIONS IN
PARENTHESES)

Ge-O(1)	1.770(7)	Li(1)/Zn(1)-O(1)	1.99(2)
Ge-O(1')	1.770(7)	Li(1)/Zn(1)-O(1')	1.99(2)
Ge-O(2)	1.75(1)	Li(1)/Zn(1)-O(2)	1.85(4)
Ge-O(3)	1.74(1)	Li(1)/Zn(1)-O(3)	2.13(4)
Mean	1.76	Mean	1.99
Li/Zn(2)-O(1)	1.87(5)	Li(2a)-O(1)	1.84(8)
Li/Zn(2)-O(1')	2.05(4)	Li(2a)-O(1')	2.42(8)
Li/Zn(2)-O(2)	1.92(4)	Li(2a)-O(2)	2.04(7)
Li/Zn(2)-O(3)	2.00(4)	Li(2a)-O(3)	1.79(7)
Mean	1.96	Mean	2.02
Li(3)-O(1'')	2.11(4)	Li(4)-O(1)	2.120(7)
Li(3)-O(1''')	2.11(4)	Li(4)-O(1')	2.120(7)
Li(3)-O(3)	2.31(6)	Li(4)-O(3)	2.074(5)
Li(3)-O(1')	2.46(5)	Li(4)-O(3')	2.074(5)
Li(3)-O(1)	2.46(5)	Li(4)-O(2)	2.468(7)
Li(3)-O(2)	2.60(7)	Li(4)-O(2')	2.468(7)

0.75 compared to $x = 0.5$, may be accounted for by the greater level of impurities in this profile.

Discussion

Both $\text{Li}_3\text{Zn}_{0.5}\text{GeO}_4$ and $\text{Li}_{3.5}\text{Zn}_{0.25}\text{GeO}_4$ are interstitial solid solutions based on the γ -polymorph of $\text{Li}_2\text{ZnGeO}_4$ (Fig. 3). Although this polymorph exists only at high temperatures it is assumed to be isostructural with $\gamma\text{-Li}_3\text{PO}_4$ for which structure determinations have been carried out (13, 14). The structure of $\gamma\text{-Li}_2\text{ZnGeO}_4$ consists of an oxide ion array that is between hexagonal close packing and tetragonal packing (15), with Li, Zn, and Ge ions occupying one half of the tetrahedral sites within the oxygen array. The Li^+ and Zn^{2+} ions are distributed over two sets of tetrahedral

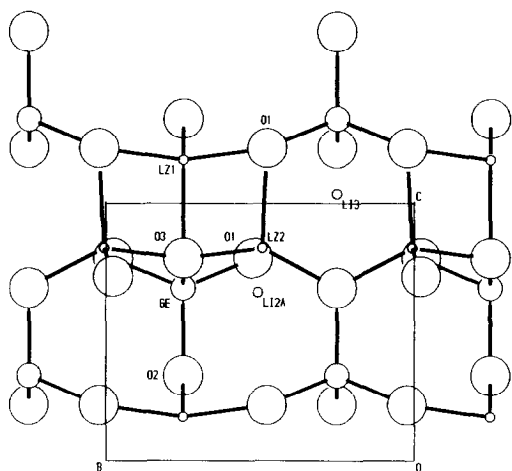
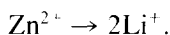


FIG. 3. View of the LISICON structure along the a axis. $\text{Li}_{3.5}\text{Zn}_{0.5}\text{GeO}_4$ composition.

sites (designated sites (1) and (2) in the tables). These tetrahedra share common edges. The GeO_4 tetrahedra on the other hand are isolated, sharing only corners with the $(\text{Li}/\text{Zn})\text{O}_4$ tetrahedra. The lithium-rich solid solutions, such as $\text{Li}_3\text{Zn}_{0.5}\text{GeO}_4$ and $\text{Li}_{3.5}\text{Zn}_{0.25}\text{GeO}_4$, are structurally somewhat similar to $\gamma\text{-Li}_2\text{ZnGeO}_4$, the principal difference being the replacement of Zn^{2+} by Li^+ according to the mechanism:



The zinc ions are replaced by lithium ions in tetrahedral sites while the additional lithium ions occupy interstitial octahedral sites. However, the distributions of tetrahedrally coordinated Li^+ and Zn^{2+} ions within the oxide ion array are not as given for the stoichiometric compound. The interstitial octahedral site Li(3) shares faces with two tetrahedral sites Li/Zn(2): examination of the data presented in Tables I and III suggest that Li^+ ions occupying site (3) displace lithium ions from site (2) through a common face into (2a) tetrahedral sites, thus avoiding the energetically unfavorable Li^+ -ion repulsions associated with simultaneous occupation of sites (2) and (3). Fur-

ther consideration of the data in Tables I and III appears to indicate that on changing the composition from $x = 0.5$ to $x = 0.75$ the zinc occupancy decreases primarily on site (2), while the lithium ion occupancy primarily increases on sites (3) and (2a).

The two types of interstitial Li ions in sites Li(3) and Li(4) are not located in regular oxygen octahedra; the oxide ion arrangement is significantly distorted such that Li(3) is preferentially coordinated to three oxygen atoms on one face of the octahedral site, while Li(4) is essentially 4-coordinate in a square planar geometry.

The refined cell parameters obtained in the present work are similar to those observed in the previous single-crystal X-ray studies by Hong (1) and Plattner and Völlenkle (5). The refined Ge and O positions were found to agree reasonably well in both the present determinations with those in the corresponding single-crystal X-ray structures. The average Ge-O bond length of 1.76 Å in both compounds is in good agreement with the average distances of 1.74 Å for $\text{Li}_3\text{Zn}_{0.5}\text{GeO}_4$ and 1.75 Å for $\text{Li}_{3.5}\text{Zn}_{0.25}\text{GeO}_4$ found previously and also with similar Ge-O systems, e.g., 1.76 Å in LiScGeO_4 (16).

The refined positions for Li/Zn(1) were also found to compare well with the previously obtained data. Both the present determinations give slightly higher Zn occupancy on site (1) than observed in the X-ray studies, although all the values lie within 2 e.s.d.s of the previously reported figures. The Li/Zn(2) sites in both of the present structures are significantly shifted from those reported by Hong and Plattner and Völlenkle. This is associated with the positional/thermal disorder, indicated previously, between sites (2) and (2a), and is reflected in the high e.s.d.s for these positions. There are two significant differences between the X-ray determined structures and the present determinations. First there is a complete absence in the former

studies of Li(2a) in both the $x = 0.5$ and the $x = 0.75$ compositions: this is compensated for in our structure determinations by a reduced occupancy of Li site (2) compared with that observed previously. Second, Hong reported lithium occupation of the octahedral site at 0, 0, 0; occupation of this site seems unlikely at ambient temperature as it is of high energy, sharing faces with two GeO_4 tetrahedra and no evidence was found in either of the present determinations for occupation of this site.

The sum of the refined Li occupancies for the structures are 2.8(1) atoms per formula unit, for $\text{Li}_3\text{Zn}_{0.5}\text{GeO}_4$, and 3.2(2) atoms per formula unit, for $\text{Li}_{3.5}\text{Zn}_{0.25}\text{GeO}_4$. Although in view of the quoted e.s.d.s these figures seem in reasonable agreement with the values anticipated from the formulas, it is possible that we have not located all the lithium ions present in the structures.

The structure of a similar γ -phase $\text{Li}_{3.4}\text{Si}_{0.7}\text{S}_{0.3}\text{O}_4$ as determined by Fitch *et al.* (17), also exhibits displacement of lithium ions into face-sharing tetrahedral sites. However, Fitch *et al.* (17) identified a finite lithium occupancy in the tetrahedral site sharing a face with Li(1).¹ No evidence was found for the occupation of the equivalent (1a) site in either of our determinations. Another interesting difference is the location of the interstitial Li; Fitch *et al.* find no occupation of site (3) instead they locate all their interstitial Li in site (4).

In summary, the Li distributions in the structures of $\text{Li}_3\text{Zn}_{0.5}\text{GeO}_4$ and $\text{Li}_{3.5}\text{Zn}_{0.25}\text{GeO}_4$ have been shown to differ signifi-

cantly from that determined previously by single-crystal X-ray diffraction. This, we believe justifies the use of the technique of powder neutron diffraction in this study.

Acknowledgments

We gratefully acknowledge the assistance of A. Hewat of the ILL (Grenoble) and the support of the SERC for this work.

References

1. H. Y.-P. HONG, *Mater. Res. Bull.* **13**, 117 (1978).
2. P. G. BRUCE AND A. R. WEST, *Mater. Res. Bull.* **15**, 379 (1980).
3. P. G. BRUCE AND A. R. WEST, *J. Solid State Chem.* **44**, 354 (1982).
4. P. G. BRUCE AND A. R. WEST, *J. Solid State Chem.* **53**, 430 (1984).
5. E. PLATTNER AND H. VÖLLENKLE, *Monatsh. Chem.* **110**, 693 (1979).
6. H. M. RIETVELD, *J. Appl. Crystallogr.* **2**, 65 (1969).
7. G. E. BACON, "Neutron Diffraction," 3rd ed., Oxford Univ. Press (Clarendon), London/New York (1975).
8. L. KOESTER AND H. RAUCH, IAEA Report 2517/RB (1981).
9. T. HAHN, Ed., "International Tables for Crystallography," Vol. A, Reidel, Dordrecht/Boston (1983).
10. J. ZEMANN, *Acta Crystallogr.* **10**, 664 (1957).
11. M. W. THOMAS AND P. J. BENDALL, *Acta Crystallogr. Sect. A* **34**, S351 (1978).
12. P. J. BENDALL, A. N. FITCH, AND B. E. F. FENDER, *J. Appl. Crystallogr.* **16**, 164 (1983).
13. J. ZEMANN, *Acta Crystallogr.* **13**, 863 (1960).
14. W. H. BAUR, *Inorg. Nucl. Chem. Lett.* **16**, 525 (1980).
15. A. R. WEST AND P. G. BRUCE, *Acta Crystallogr. Sect. B* **38**, 1891 (1982).
16. E. A. GENKINA, V. A. TIMOFEEVA, AND A. B. BYKOV, *Zh. Strukt. Khim.*, **27**(3), 167 (1986).
17. A. N. FITCH, B. E. F. FENDER, AND J. TALBOT, *J. Solid State Chem.* **55**, 14 (1984).

¹ The atomic site numeration used in the text differs from that used in Ref. (17).